2000 ASME International Mechanical Engineering Congress and Exhibit, Orland, November 5-11, 2000

MOLECULAR DYNAMICS SIMULATION OF HYDROGEN STORAGE IN SINGLE-WALLED CARBON NANOTUBES

Shigeo MARUYAMA
Engineering Research Institute
The University of Tokyo
2-11-16 Yayoi, Bunkyo-ku, Tokyo 113-8656, Japan
maruyama@photon.t.u-tokyo.ac.jp

Tatsuto KIMURA
Department of Mechanical Engineering
The University of Tokyo
7-3-1 Hongo, Bunkyo-ku, Tokyo 113-8656, Japan
kimutatu@photon.t.u-tokyo.ac.jp

ABSTRACT

The hydrogen storage mechanism of SWNTs was studied through molecular dynamics simulations. Assuming the simple physical adsorption of hydrogen to the surface of SWNTs, potential forms between H_2-H_2 and C-H_2 were both expressed by Lennard-Jones functions. Fixing the relative coordinates of carbon atoms to the center of mass of each SWNT, the center of mass motion was modeled with the van der Waals force between SWNTs. Hydrogen absorption in small bundles of (8,8), (10,10) and (12,12) SWNTs were tested. In order to realize the adsorption between SWNTs within reasonable simulation period, the van der Waals energy between tubes was once decreased and recovered. While the amount of hydrogen adsorption per unit carbon mass *inside* SWNTs increased with increasing diameter, adsorption *between* tubes was almost constant. Total amount of hydrogen adsorption for 77 K and 15 MPa system was predicted as 6.9, 7.7, and 8.1 wt % for (8,8), (10,10), and (12,12) bundles, respectively.

INTRODUCTION

Dillon et al. [1] suggested the possibility of achieving very high hydrogen storage capacity per unit mass by using single-walled carbon nanotubes (SWNTs), as hydrogen supply source of the fuel cell for automobiles. SWNTs, originally discovered by Iijima [2], can now be efficiently produced by such techniques as laser-vaporization in high temperature oven [3] and the arc-discharge method [4]. By experiments using relatively high-purity SWNTs, hydrogen storage capacity of about 8 % at 80 K and 120 atm was reported by Ye et al. [5], and about 4.2 % at room temperature and 100 atm was reported by Liu et al. [6]. One the other hand, the hydrogen adsorption characteristics were examined by molecular simulations using the Monte Carlo method [Wang and Johnson [7] and Darkrim and Levesque [8]]. However, there are still many unknown questions on the mechanism of such efficient hydrogen storage. It is still argued whether the adsorption to the interior of SWNT or outside is more important, and whether it is simply physical adsorption or some chemical reaction is being involved. In this study, the physical adsorption of hydrogen molecules to a small bundle of SWNTs was simulated by the molecular dynamics method. A special attention was paid to the intrusion of hydrogen molecules in-between the SWNTs by broadening the spacing of each SWNT. The relaxation of the energy parameter of van der Waals potential between SWNTs was necessary for the simulation of the hydrogen intrusion within the reasonable simulation period. Through a separate simpler simulation, the amount of hydrogen absorption interior of each SWNT was calculated. Finally, the predicted capacity of total hydrogen storage was compared with experiments.

NOMENCLATURE

$\boldsymbol{A}$:	Unit crystal vector
d_0:	Diameter of a SWNT
E_c:	Cohesive energy per carbon atom
m:	An integer
n:	An integer
N:	Number of molecules
p:	Pressure
R:	Distance between two SWNTs
r:	Distance between two molecules
T:	Temperature
U:	Potential energy

Greek Symbols

α: Relaxation parameter of tube-tube potential
ε: Energy parameter of Lennard-Jones potential
σ: Length parameter of Lennard-Jones potential

Subscripts
A: Adsorbed
C: Carbon
HC: Between hydrogen and carbon
HH: Between hydrogen molecules
in: Interior of SWNT
TT: Between SWNTs
out: Outside of SWNT

SIMULATION METHOD

As for the hydrogen molecule, when the molecular mass is small and when temperature is low, it is known that quantum effect becomes remarkable in the trajectory of molecules. When we consider the hydrogen supply source of fuel cell for automobiles, it is difficult to consider the utilization of lower temperature than the liquid nitrogen temperature, 77K. Then, the quantum effect is expected to be relatively small as in the results of path integral molecular dynamics simulation by Wang and Johnson [7]. Hence, for the simplicity and for gaining a larger system size, we disregarded the quantum effect in this study and classically handled hydrogen molecules. In addition, intra-molecule vibration and rotation of a hydrogen molecule were also neglected. The intermolecular potential function of hydrogen molecules was approximated by following Lennard-Jones (12-6) potential, with classically known parameters: ε_{HH} = 3.180 meV, σ_{HH} = 2.928 Å.

$$U = 4\varepsilon\left\{\left(\frac{\sigma}{r}\right)^{12} - \left(\frac{\sigma}{r}\right)^{6}\right\} \quad (1)$$

The interaction of a hydrogen molecule and a carbon atom in SWNT is rather difficult to estimate. As the first order approximation, we simply employed Lennard-Jones (12-6) function between a hydrogen molecule and a carbon atom of the graphite. Referring to adsorption experiments of hydrogen molecule to the graphite, potential parameters were set as: ε_{HC} = 2.762 meV, σ_{HC} = 3.179 Å.

The geometrical structure of a SWNT, i.e. diameter and chirality, can be determined by an index (n, m), where n and m are integers [e.g. Dresselhaus & Dresselhaus [9]]. It can be imagined that a geometrical structure of SWNT is obtained by curling a graphite sheet in such a way that a hexagon in the edge of the graphite surface will meet another hexagon. Regarding that the center of one hexagon is origin, the position of the center of another hexagon in the original flat sheet is expressed as $n\mathbf{A}_1+m\mathbf{A}_2$. Here, $\mathbf{A}_1$ is a unit crystal vector from the origin to the center of a neighbor hexagon, and $\mathbf{A}_2$ vector is directed to the center of another neighbor hexagon with a 60° angle with $\mathbf{A}_1$. A SWNT with an index (n, n) is called armchair type from the geometrical feature in longitudinal cut section as shown in Figure 1. Among the infinitely possible choices of (n, m), the

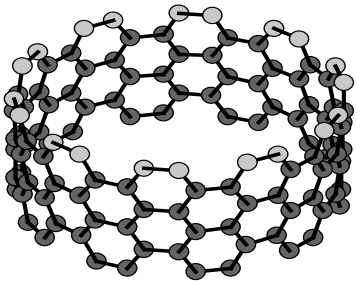

Fig. 1 Structure of (10,10) SWNT.

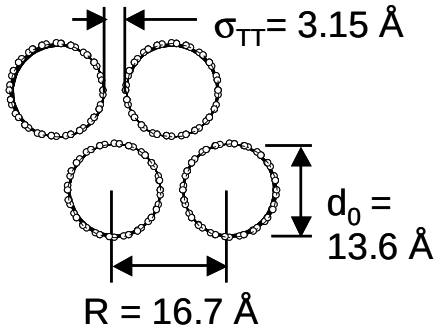

Fig. 2 Minimum energy structure of a bundle of (10,10) SWNTs.

Table 1 Potential parameters between SWNTs

Tube	d_0 [Å]	σ_{TT} [Å]	ε_{TT} [meV/Å]	E_c [meV]	N_C
(8, 8)	10.856	3.157	79.19	18.27	448×7
(10, 10)	13.570	3.149	89.50	16.52	560×7
(12, 12)	16.283	3.147	98.88	15.21	672×7

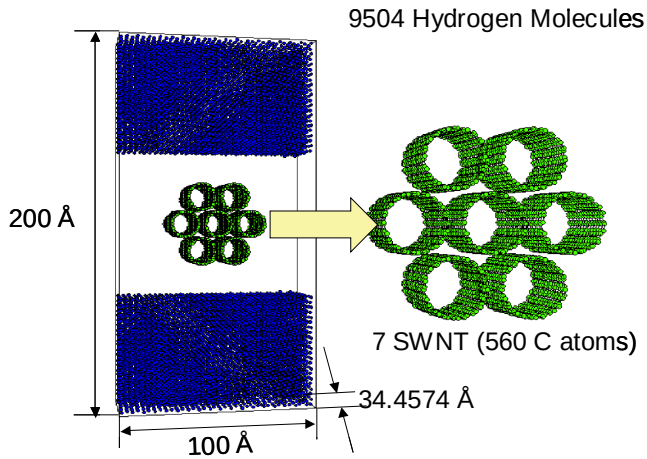

Fig. 3 Initial configuration for (10,10) SWNTs.

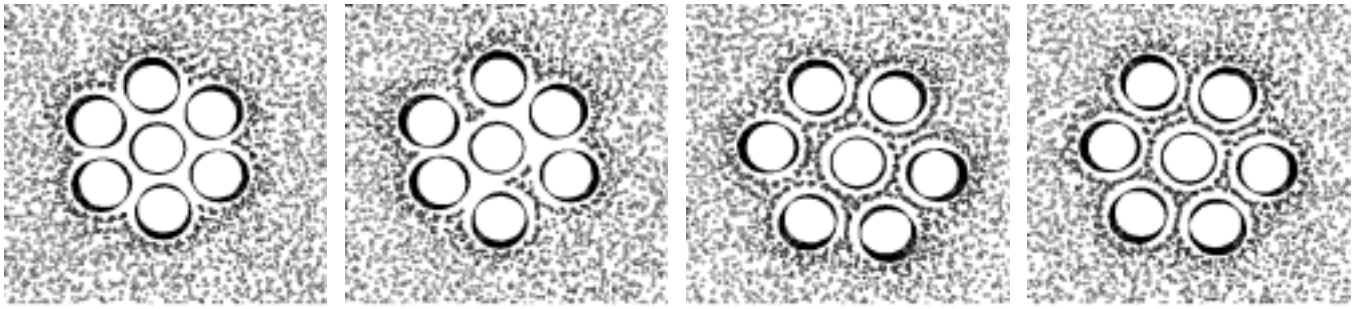

(a) (10,10) 500 ps (b) (10,10) 510 ps (c) (10,10) 1000 ps (d) (10,10) 1500 ps

Fig. 4 Adsorption of hydrogen molecules between SWNTs. SWNTs are shown as bond lines. (a) No intrusion, $\alpha = 1$; (b) During intrusion, $\alpha = 0.02$; (c) Stable absorption, $\alpha = 0.02$; (d) Final, $\alpha = 1$.

(10,10) structure shown in Figure 1 is well known by the experimental speculation by Thess et al. [3]. Another quite symmetric structure is obtained by (n,0) which is called zigzag type. In this study, the following 3 armchair type structures were compared: (10,10) in Figure 1, (8,8), and (12,12) with different diameters

By disregarding the vibrational motion between carbon atoms in a nanotube, a SWNT was regarded as one large rigid molecule. Then, the potential function between SWNTs was determined by the following procedure. By decomposing the van der Waals interaction of graphite sheets, the van der Waals force between two carbon atoms was expressed in Lennard-Jones (12-6) potential as: ε_{CC} = 2.40 meV, σ_{CC} = 3.37 Å. Assuming the additive nature of van der Waals potential, the effective potential between two SWNTs was obtained as the summation of potentials for all combination of carbon atoms. The calculated effective potential was very nicely fit by the Lennard-Jones type (8,4) function in the following equation.

$$U_{TT} = \alpha\varepsilon_{TT}\left\{\left(\frac{\sigma_{TT}}{(R-d_0)}\right)^8 - 2\left(\frac{\sigma_{TT}}{(R-d_0)}\right)^4\right\} \qquad (2)$$

Here, σ_{TT} is the potential length scale between tubes, as shown in Figure 2, d_0 is diameter of SWNT, and ε_{TT} is the energy scale for unit length of a SWNT. An optional coefficient α, relaxation parameter, was unity for the potential fittings. This parameter α was modified in the range $(0 < \alpha \le 1)$ in order to imaginary reduce the van der Waals force between tubes. The determined potential parameters for different types of SWNTs are listed in Table 1. Here, the cohesive energy per carbon atom E_c was almost the same as the estimation by Tersoff & Ruoff [10]. Though power indexes of 8 and 4 in the function of equation (2) were originally determined for the best fit of the effective potential through 'try and error' procedures, a logical explanation can be possible as follows. Since the repulsive force is short-range, repulsive interaction of two SWNTs is similar to the interaction between two 2-D planes. Hence, the 4 folds integration of the repulsive term $(\sigma_{CC}/r)^{12}$ gives the power of 8. On the other hand, when dealing with the long-range attractive force, the interaction is closer to line-to-line

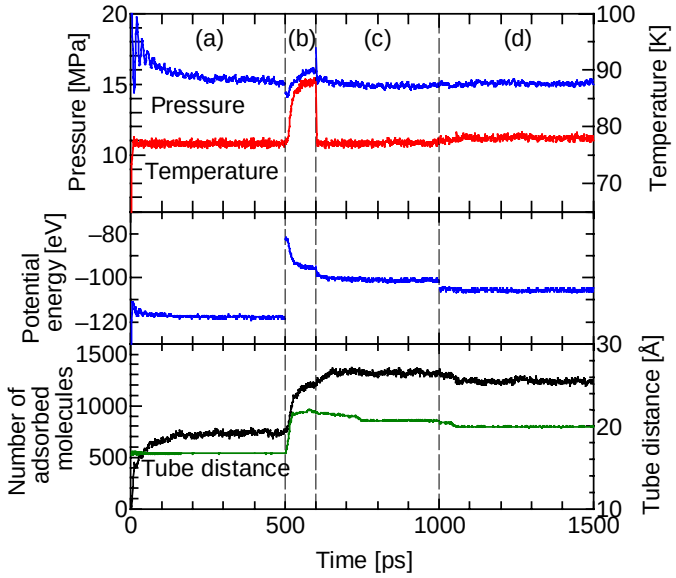

Fig. 5 Adsorption between (10,10) SWNTs. (a) $\alpha = 1$, T: const., (b) $\alpha = 0.02$, (c) $\alpha = 0.02$, T: const., (d) $\alpha = 1$.

alignment, which gives the double integration of $(\sigma_{CC}/r)^6$ term to result the power of 4.

As shown in Figure 3, 7 SWNTs were placed in a fully periodic system with 100 × 34.4574 × 200 Å, so that a SWNT exactly continues in the longitudinal direction. Since the experimentally observed SWNTs had longitudinal length of 10 to 100 μm [3], we preferred to model the infinitely long tubes. The hydrogen adsorption interior of each SWNT was calculated separately by a bit shorter SWNTs, so that hydrogen molecules could freely access to the tube interior. Hydrogen molecules were initially placed as fcc structure at top and bottom of SWNTs as in Figure 3. The Verlet's leap-frog method was used for the numerical integration of equation of motion with the time step of 5 fs. The temperature control by the velocity scaling was used when it was necessary.

Table 2 Final amount of hydrogen absorption

Tube	p [MPa]	U [eV]	r [Å]	Outside N_{Aout}	Interior N_{Ain}/N_C	Total [wt %]
(8, 8)	15.0	-97.6	16.8	980	32/320C	6.88
(10, 10)	15.1	-105.6	20.0	1240	57/400C	7.65
(12, 12)	15.5	-116.0	22.3	1430	88/480C	8.12

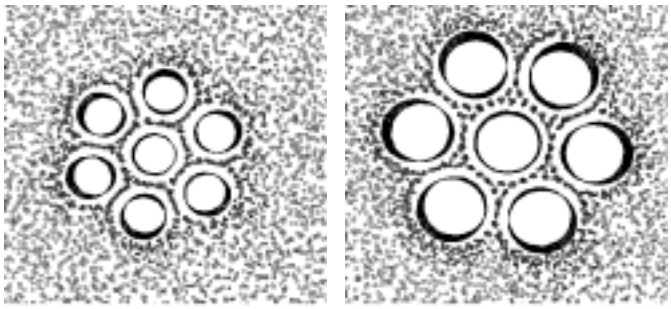

(a) (8,8) 1500 ps (b) (12,12) 1500ps

Fig. 6 Adsorption of hydrogen molecules for SWNTs with different diameters. SWNTs are shown as bond lines and carbon atoms are not shown.

RESULTS AND DISCUSSIONS

Figure 4 shows the representative snapshots of the adsorption process for (10,10) SWNTs in correspondence to the time history of temperature, pressure, potential energy, number of adsorption molecules, and average distance between SWNTs in Figure 5. Here, the carbon atoms are not shown for clarity. The normal hydrogen adsorption process for the condition of liquid nitrogen temperature, 77K, and about 150 atm is shown in Figure 4(a) and Figure 5(a). Here, the velocity scaling was used to keep the hydrogen temperature. During 500 ps, the adsorption was observed only outside of a bundle. It was expected that even if the minimum energy structure consisted of hydrogen molecules between SWNTs, the time scale we needed to wait might be much longer than we could handle with the molecular dynamics simulations. Then, the relaxation parameter α was reduced to 0.02 in order to reduce the van der Waals force between SWNTs. Then, the hydrogen molecules rapidly intruded into between SWNTs by expanding the bundle of SWNTs as shown in Figure 4(b) and 5(b). Here, the sudden jump in the potential energy was due to the sudden decrease of van der Waals interaction. Since the temperature control was not used in this period [Figure 5(b)], the temperature rise by heat of adsorption and the pressure increase due to the temperature rise were recorded in Figure 5(b). After turning on the temperature control in Figure 5(c), the mean distance between SWNTs settled down at about 20.0 Å, and there was 1 or 2 layers of hydrogen molecules between SWNTs as in Figure 4 (c). Finally, as the relaxation parameter was restored to $\alpha = 1$, there was hardly the change in the adsorption structure as in Figure 4(d). This relaxation technique might be considered that the potential barrier to be overcome for the kind of phase-transition was artificially lowered to accelerate the transition. However, the modification of α was not as simple as just increasing the probability of the transition, but it promoted the one-way transition. Even if we could restore α to 1 without the change in the structure, it was not possible to conclude that the structure with hydrogen between tubes was more stable. Probably some thermodynamics considerations with free energy aspects of the system are necessary for the more elaborate discussion.

(a) (8,8) (b) (10,10) (c) (12,12)

Fig. 7 Hydrogen storage inside each SWNT. SWNTs are shown as bond lines.

The same procedures of simulations as for (10,10) structure were repeated for (8,8) and (12,12) as shown as the final structures in Figure 6. In case of (12,12) system, however, no hydrogen intrusion between SWNTs were observed within about 500 ps with $\alpha = 0.02$. Then, we needed to further decrease the van der Waals force to $\alpha = 0.01$. Otherwise the same procedures as the case of (10,10) were performed. The number of finally adsorbed hydrogen molecules N_{Aout} is listed in table 2 in comparison with pressure p and potential energy U. Here, N_{Aout} was almost proportional to the number of carbon atoms N_C at least among these 3 kinds of nanotubes. Hence, the amount of hydrogen per unit carbon mass became about 5.2 wt % regardless of the tube diameter. It is very straightforward to understand this result: the number of absorbed hydrogen molecules in exterior of SWNTs was simply proportional to the exterior surface area of SWNTs.

There is wide-open space in interior of SWNTs. Usually the both ends of as-grown SWNTs are capped with semi-fullerene structure. However, the space in the interior of SWNT is also available for hydrogen storage, if fullerene cap of the nanotube tip is opened. The oxidization technique and the chemical treatments are known to open up this fullerene caps. In order to estimate the absorption amount to the tube interior, a bit shorter SWNTs that did not continue in the periodic boundary was simulated. Figure 7 shows the final absorbed

structure for about 150 atm and 77 K. The number of absorbed hydrogen molecules N_{Ain} compared with the number of carbon atoms N_c for these shorter SWNTs are also listed in Table 2. Number of absorbed hydrogen molecules relative to the number of carbon atoms N_{Ain}/N_c is directly proportional to the weight percent. Hence, the increase in diameter of SWNT increases the effectiveness of interior space for absorption. The total absorption amount of hydrogen in weight percent is listed in Table 2. As a result, SWNTs with larger diameter had an advantage for total hydrogen storage capacity. This result is consistent with the speculations of Dillon et al. [1]. The predicted amount of hydrogen absorption is almost in good agreement with the experimental value by Ye et al. [5]. It is concerned, however, this almost perfect agreement may be just a coincidence, because of the simplicity of our model system.

CONCLUSIONS

The hydrogen storage mechanism of SWNTs was studied through molecular dynamics simulations. The intrusion of hydrogen molecules in-between SWNTs by broadening the spacing of each SWNT was simulated by temporally decreasing the van der Waals potential between SWNTs. While the amount of hydrogen adsorption *inside* SWNTs increased with increasing diameter, adsorption *between* SWNTs was almost constant. Total amount of hydrogen adsorption for 77K and 15 MPa system was predicted as 6.9, 7.7, and 8.1 wt % for (8,8), (10,10), and (12,12) bundles, respectively.

ACKNOWLEDGEMENT

Part of this work was supported by Grant-in-Aid for Scientific Research (B) (No. 12450082) from the Ministry of Education, Science, Sports and Culture, Japan.

REFERENCES

1. Dillon, A. C., Jones, K. M., Bekkedahl, T. A., Kiang, C. H., Bethune, D. S., and Heben, M. J., 1997, "Storage of Hydrogen in Single-Walled Carbon Nanotubes," *Nature*, vol. 386-27, pp. 377-379.
2. Iijima, S. and Ichihashi, T., 1993, "Single-Shell Carbon Nanotubes of 1 nm Diameter," Nature, vol. 363, pp.603-605.
3. Thess, A., Lee, R., Nikolaev, P., Dai, H., Petit, P., Robert, J., Xu, C., Lee, Y. H., Kim, S. G., Rinzler, A. G., Colbert, D. T., Scuseria, G. E., Tomának, D., Fischer, J. E., and Smalley, R. E., 1996, "Crystalline Ropes of Metallic Carbon Nanotubes," Science, vol. 273, pp. 483-487.
4. Journet, C., Maser, W. K., Bernier, P., Loiseau, A., de la Chapelle, M. L., Lefrant, S., Deniard, P., Lee, R., Fisher, J. E., 1997, Nature, vol. 388, pp. 756.
5. Ye, Y., Ahn, C. C., Witham, C., Fultz, B., Liu, J., Rinzler, A. G., Colbert, D., Smith, K. A., and Smalley, R. E., "Hydrogen Adsorption and Cohesive Energy of Single-Walled Carbon Nanotubes," 1999, *Appl. Phys. Lett.*, vol. 74-16, pp. 2307-2309.
6. Liu, C., Fan, Y. Y., Liu, M., Cong, H. T., Cheng, H. M., and Dresselhaus, M. S., 1999, "Hydrogen Storage in Single-Walled Carbon Nanotubes at Room Temperature," *Science*, vol. 286-5, pp. 1127-1129.
7. Wang, Q. and Johnson, J. K., 1999, "Molecular Simulation of Hydrogen Adsorption in Single-Walled Carbon Nanotubes and Idealized Carbon Carbon Slit Pores," *J. Chem. Phys.*, vol. 110-1, pp. 577-586.
8. Darkrim, F. and Levesque, D., 1998, "Monte Carlo Simulations of Hydrogen Adsorption in Single-Walled Carbon Nanotubes," *J. Chem. Phys.*, vol. 109-12, pp. 4981-4984.
9. Dresselhaus, M. S. and Dresselhaus, G., 1996, *Science of Fullerenes and Carbon Nanotubes*, Academic Press, p. 144.
10. Tersoff, J. and Ruoff, R. S., 1994, "Structural Properties of a Carbon-Nanotube Crystal," Phys. Rev. Lett., vol. 73-5, pp. 676-679.